Adaptive Control of a Serial-in-Parallel Robotic Rehabilitation Device

Ali Utku Pehlivan, *Student Member, IEEE,* Fabrizio Sergi, *Member, IEEE,*
Marcia K. O'Malley, *Member, IEEE*

***Abstract*— Robotic rehabilitation is an effective platform for sensorimotor training after neurological injuries. In this paper, an adaptive controller is developed and implemented for the RiceWrist, a serial-in-parallel robot mechanism for upper extremity robotic rehabilitation. The model-based adaptive controller implementation requires a closed form dynamic model, valid for a restricted domain of generalized coordinates. We have used an existing method to define this domain and verify that the domain is widely within the range of admissible tasks required for the considered application (movements-based wrist and forearm rehabilitation). Simulation and experimental results that compare the performance of the adaptive controller to a proportional- derivative controller show that the trajectory tracking performance of the adaptive controller is better compared to the performance of a PD controller using the same values of feed- back gains. Further, comparable absolute error performance is obtained with the adaptive controller for feedback gains nearly one third that required for the PD controller. With the lower gains used in the adaptive controller, good tracking performance is achieved with a more compliant controller that will allow the subject to indicate their ability to independently initiate and maintain movement during a rehabilitation session.**

I. Introduction

Rehabilitation of patients with impairments due to neurological lesions, including stroke and spinal cord injury, mostly includes repetitive movements which are known to improve muscle strength and movement co-ordination [1]. The goal of neurorehabilitation is to improve functional outcomes by promoting plasticity in the brain and spinal cord. To fulfill this goal, therapy has to be intensive with long duration and high repetition numbers.

Robotic devices are well-suited to rehabilitation after stroke and SCI because they can ensure consistency of therapeutic interactions at high intensity and repetitions. Robotic systems also enable the objective and quantitative performance evaluation of patients both during and after the therapy sessions.In addition, virtual reality implementations can provide a unique medium where therapy can be provided within a functional and highly motivating context [2], and consequently the intensity of the therapy can be increased. Indeed the results of clinical studies involving robotic rehabilitation protocols support the idea of implementing these devices in treatment of stroke [3] and SCI patients [4].

A critical area of research in rehabilitation robotics is the development of control algorithms able to regulate the interaction between the device and the patient, so that the selected exercises can promote motor plasticity, and therefore improve motor recovery [5]. The differences among assisting control applications mainly arises at the degree of assistance. Lum et al. [6] used the MIME upper extremity rehabilitation robot for shoulder and elbow neurorehabilitation in subacute stroke patients, using a position control assistance strategy. This control strategy led to improvements in physical performance and motor learning, compared to the control groups, for subacute stroke patients [6] and with unimpaired patients [7]. Despite these positive outcomes, it was shown that in chronic patients, passively moving patients' limbs with a robotic device does not contribute to recovery, suggesting that recovery requires active participation [8]. An alternative strategy is triggered assisting control, in which the movement is initiated by the patient according to a predefined measure (such as a force/torque threshold), and the robotic device provides assistance for the rest of the movement [9]. Although this approach increases the participation of patient during the subject-driven part, during some phases of the interaction the patient is completely passive [10].

Because fixed gain controllers may provide more assistance than is needed by the patient, researchers have begun to develop assist-as-needed controllers [5]. Such a controller adapts its parameters based on online measurement of the patient's performance. For example, Wolbrecht et al. [11] developed an assist-as-needed control algorithm which consisted of two main parts: a passivity based adaptive controller and a forgetting term that reduced progressively robot contribution to movements, so to promote subjects' active participation. The main idea behind choosing an adaptive controller was to be able to model both the dynamics of the orthosis, and the patient's ability and effort. Hence the controller would provide necessary torque to complete the movement with an increased mechanical compliance. This controller was implemented on Pneu-WREX [12], a pneumatically actuated, 4 degree-of-freedom (DOF), serial mechanism.

In this paper, we present the implementation of this adaptive controller on RiceWrist [13] (Fig. 1(b)), an electrically actuated, 4 DOF serial-in-parallel mechanism. The trajectory tracking performance of the controller is compared to performance of a fixed gain PD controller both in simulation and experimentally on the RiceWrist hardware.

II. Methods

RiceWrist [13], is a wrist and forearm exoskeleton device; its basic kinematic structure is depicted in Fig. 1(a). The exoskeleton is comprised of a revolute joint for forearm rotation, in series to a 3-RPS (revolute-prismatic-spherical)

The authors are with the Mechatronics and Haptic Interfaces Laboratory, Department of Mechanical Engineering and Materials Science, Rice University, Houston, TX 77005 (e-mails: aliutku@rice.edu, fabs@rice.edu, omalleym@rice.edu)

978-1-4673-6024-1/13/$31.00 ©2013 IEEE

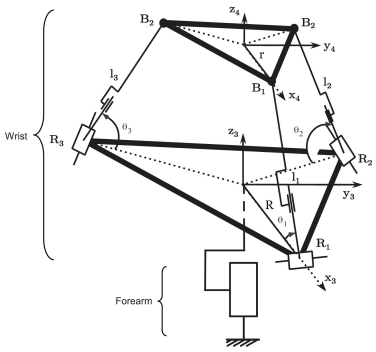

(a)

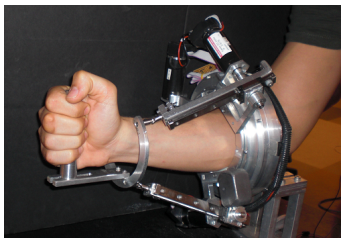

(b)

Fig. 1. (a) 4 DOF RiceWrist employs a 3-RPS (revolute-prismatic-spherical) parallel mechanism at the wrist module and a revolute joint at the forearm (b) The physical hardware.

parallel wrist. The first DOF corresponds to forearm rotation, while the two rotational DOFs of the robotic wrist correspond to wrist flexion/extension and abduction/adduction. The dynamic equations of the system can be given as

$$M(q)\ddot{q} + C(q,\dot{q})\dot{q} + G(q) = F_r + J^T F_p \qquad (1)$$

where q is a 4×1 vector of joint variables, M is the 4×4 inertia matrix, C is the 4×4 matrix which represents Coriolis/centrifugal terms, G is the 4×1 gravity vector, F_r is the 4×1 vector of forces applied by the actuators and F_p is the 4×1 vector of forces applied by patient at the end-effector (handle).

Because the system employs a closed-chain parallel mechanism, and because of the implicit nature of the loop equations, representing the equations of motion in the form of Equation 1 is not straightforward [14]. However, using the formulation in [15], it can be shown that the dynamical equations of the RiceWrist can be expressed in the form of Equation 1 and posses identical properties as open-chain serial mechanisms. The important distinction, however, is that the given dynamical model is valid only locally, i.e. the domain of the generalized coordinates (q) is a bounded and closed set ($\mathbf{\Omega}$) rather than the whole n-dimensional real space (n corresponds to the number of DOF of the device, in our case $n = 4$) [15]: $q \in \ \Omega$, where $\Omega \subset \Re^n$.

Consequently, it can be said that the 4-DOF serial-in-parallel mechanism possesses the two important properties, of skew-symmetry [16], and linearity-in-the-parameters [17].

A multitude of model-based control schemes has been developed and applied to robotic systems described by Equation 1 and their global stability has been proved exploiting also the two properties described above. However, in order to develop adaptive controllers for systems with parallel chains, it is necessary to accurately define the domain of the workspace of the parallel mechanism in which local stability can be proved and to guarantee that the system is always within this range during operation.

A. Domain of validity of the reduced model

In this paper, we will follow the modeling approach described in [15], which is based on cutting-open a generic parallel chain in a sub-set of rigid bodies or serial structures, described in terms of n' generalized coordinates q' ($n' > n$). In the parallel structure, such coordinates satisfy a set of $n' - n$ constraint equations, that for a holonomic system can be written in the form:

$$\phi(q') = 0. \qquad (2)$$

This implies that the generalized coordinates q' are not in general independent, but are restricted to a subspace of $\Re^n$, namely to the domain $\mathbf{U}' = \{q' \in \Re^{\mathbf{n}} : \phi(q') = 0\}$ and are named *dependent generalized coordinates*.

Normally, it is possible to choose a set of n independent generalized coordinates q among the n' coordinates q'. In this case, the mapping between q and q' can be expressed by a selection function such that $q = \alpha(q')$. Combining this result with (2), the complete kinematic model of the parallel manipulator can be expressed as:

$$\begin{bmatrix} \phi(q') \\ \alpha(q') \end{bmatrix} = \psi(q') = \begin{bmatrix} 0 \\ q \end{bmatrix} \qquad (3)$$

Accordingly, we can define the Jacobian matrix applied to the generalized model as:

$$\psi_{q'}(q') = \frac{\partial \psi}{\partial q'} \qquad (4)$$

Since a complete, closed-form kinematic model is not available for the considered system, an iterative routine is implemented to obtain the entire generalized kinematic status of the manipulator. It is possible to define the error between a measured pose (defined in terms of generalized variables q) and the calculated pose (defined in terms of q') as:

$$\overline{\psi}(q,q') = \begin{bmatrix} \phi(q') \\ \alpha(q') \end{bmatrix} - \begin{bmatrix} 0 \\ q \end{bmatrix} \qquad (5)$$

and $\overline{\psi}_{q'}(q')$ analogously as in (4).

Under the described formalism, the method described in [15] allows to estimate the size of the region of validity of the reduced model. Its main results can be summarized as follows. We start by defining $\mathbf{D}'$ as a closed rectangular interval in $\Re^{n'}$ where either the constraint functions are not satisfied, or

$$||\overline{\psi}_{q'}(q')^{-1}|| \leq c_1. \qquad (6)$$

It can be demonstrated that given $q'_\star \in \mathbf{D}'$, if $\phi(q'_\star) = 0$, then the closed sphere $B_r(q_\star)$ defined in the domain of independent generalized coordinates, with radius r, centered

around the initial point $q_\star$ is such that every point in $B_r(q_\star)$ verifies the following constraint:

$$|||[\overline{\psi}_{q'_\star}]^{-1}[\overline{\psi}_{q'} - \overline{\psi}_{q'_\star}]|| \leq \zeta_1 < 1. \tag{7}$$

The radius r, where the described reduced model is valid, can be calculated as:

$$r = \frac{\zeta_1(1-\zeta_1)}{c_1^2 c_2}, \tag{8}$$

where the constant c_2 is given by:

$$c_2 = ||B||, \tag{9}$$

and B is a matrix of elements $b_{i,j}$ that can be obtained by maximizing the derivative of the Jacobian matrix with respect to specific generalized coordinates:

$$\left\| \frac{\partial[\overline{\psi}_{q'}]_{i,j}}{\partial q'} \right\| \leq b_{i,j}. \tag{10}$$

This allows to define the domain in which the mapping between dependent and independent generalized coordinates can be applied as an invertible diffeomorphism thus allowing to model the system in the form (1). However, another result in [18] shows that this domain can be extended for a generic trajectory in $\mathbf{D}$, if it is discretized with a sufficiently small step size. In particular, if the trajectory $q_{des}(t)$ is defined in actuated joints coordinates q so that

$$q_{des}(t_i) - q_{des}(t_{i+1}) \leq r \tag{11}$$

then the domain of existence of the reduced model is extended to the whole trajectory $q_{des}(t)$. In other words, given a minimum control sampling rate, this relation poses a constraint on the maximum desired velocities for actuated joints.

The described method has been applied to the parallel portion of the RiceWrist. The following constraint equations were determined, based on the vector loop equations (ref. to Fig. 1(a)).

$$\overrightarrow{O_4R_1} + \overrightarrow{R_1B_1} + \overrightarrow{B_1O_3} = \overrightarrow{O_4O_3} \tag{12}$$
$$\overrightarrow{O_4R_2} + \overrightarrow{R_2B_2} + \overrightarrow{B_2O_3} = \overrightarrow{O_4O_3} \tag{13}$$
$$\overrightarrow{O_4R_3} + \overrightarrow{R_3B_3} + \overrightarrow{B_3O_3} = \overrightarrow{O_4O_3} \tag{14}$$

The derivatives of Equations 12-14 have been obtained in a symbolic form and the constants c_1 and c_2 have been calculated as described in Equations 6 and 9 and are shown in Fig. 2 as a function of the orientation of the RiceWrist.

It can be seen that the maximum value of constants c_1 and c_2 strongly depends on the specific extent of the workspace in which those constants are calculated. Considering as an example the domain consisting of 1-D movements (rotation along the x_4-axis which corresponds to wrist flexion-extension), it is possible to estimate a radius of validity of the reduced model equal to 1×10^{-3}, expressed as a function of normalized actuated links length (refer to [13] for a detailed description of the RiceWrist kinematic model). This radius of validity poses a constraint on the maximum admissible velocity in a 1-D flexion-extension

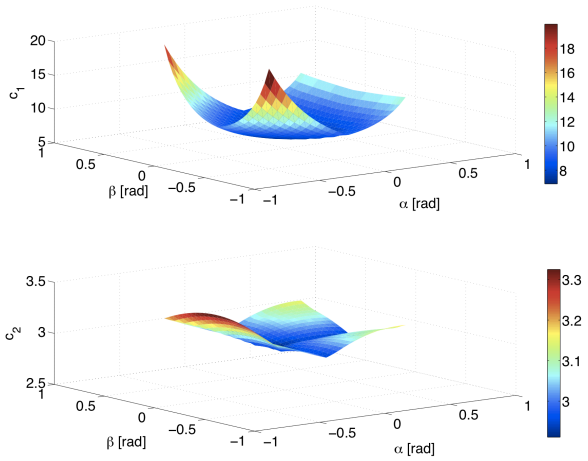

Fig. 2. Calculation of constants c_1 and c_2 as a function of end-effector coordinates. α represents radial-ulnar deviation, while β represents flexion/extension angle.

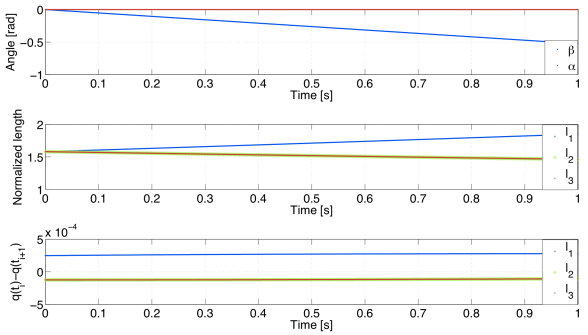

Fig. 3. Inverse kinematics for a constant-velocity movement requiring a transition from 0 to -30 deg of flexion-extension in 1 s, using a 1 ms discretization time. The necessary maximum change in actuated links length is equal to 2.7×10^{-4} (3.7 times lower than the calculated radius), implying that the same trajectory can be theoretically resampled to occur in a duration of 0.27 s with the same sampling frequency (1 kHz), still respecting condition (11) for this particular task.

movement as shown in the numerical example reported in Fig. 3, where a constant-velocity flexion-extension profile is imposed (transition from 0 to 30 deg in 1 s), and the resulting normalized actuated links lengths are calculated. It can be seen that the maximum reachable velocity for a 1-D rotation (30 deg change in end-effector rotation in 0.27 sec, or 111 deg/s peak velocity) is much higher than the range compatible with wrist rehabilitation therapy, thus validating the proposed reduced model for dynamical modeling and control of the RiceWrist for rehabilitation tasks.

B. Adaptive controller theory

We now present the adaptive controller which is based on the control algorithm developed by Slotine and Li [17]. We adopt the formulation presented in [19] and [16] which exploit the passivity property of the robotic devices.

In our formulation, we develop the controller in task space, rather than in joint space. This approach is selected because we wish to abide by the formulation in [11] which makes it

more clear to follow the construction of the regressor matrix (refer to Equation 19-21 and Equation 29). The construction of the regressor matrix is an integral step in the construction of the controller.

Let us first define the dynamic equations of the system as

$$M_T(x)\ddot{x} + C_T(x,\dot{x})\dot{x} + G_T(x) = F_r + F_p \qquad (15)$$

where x is a 4×1 vector of end effector position. M_T, C_T and G_T are the 4×4 inertia matrix, the 4×4 Coriolis/centrifugal terms matrix, and the 4×1 gravity vector, respectively, which all consist of functions of either end effector position x or velocity $\dot{x}$. The subscript T specifies that the given entities are expressed in task space, in contrast to the representation given in Equation 1. F_r is now the 4×1 vector of forces applied by the actuators which is mapped to the task space by the transpose of the Jacobian of the mechanism, and F_p is the 4×1 vector of forces applied by patient at the end-effector (handle).

Let us define the tracking error as $\tilde{x}(t) = x(t) - x_d(t)$, where $x(t)$ is 4×1 actual joint position, and $x_d(t)$ the desired trajectory which is at least twice differentiable. Both $x(t), x_d(t)$ are defined such that the corresponding joint variables $q(t), q_d(t) \in \Omega$ such that Equation 15 is valid. Consider the following control law:

$$F_r = \hat{M}_T(x)a + \hat{C}_T(x,\dot{x})v + \hat{G}_T(x) - \hat{F}_p - K_D r \qquad (16)$$

where $\hat{M}_T$, $\hat{C}_T$ and $\hat{G}_T$ are the estimates of the dynamics of the system, $\hat{F}_p$ is the estimate of the forces coming from the patient, K_D is a symmetric positive definite feedback gain matrix, and

$$\begin{aligned} r &= \dot{\tilde{x}} + \Lambda\tilde{x} = (\dot{x} - \dot{x_d}) + \Lambda(x - x_d) \\ v &= \dot{x_d} - \Lambda\tilde{x} = \dot{x_d} - \Lambda(x - x_d) \\ a &= \dot{v} \end{aligned} \qquad (17)$$

where Λ is a 4×4 constant, positive definite, symmetric matrix. Note that the desired position, velocity and acceleration are all bounded. The substitution of control input into Equation 15 will bring

$$\begin{aligned} &M_T(x)\ddot{x} + C_T(x,\dot{x})\dot{x} + G_T(x) - F_p \\ &= \hat{M}_T(x)a + \hat{C}_T(x,\dot{x})v + \hat{G}_T(x) - \hat{F}_p - K_D r \end{aligned} \qquad (18)$$

As stated above, the system dynamics are linear in terms of system parameters, and they can be modelled as

$$Y\hat{b} = \hat{M}_T a + \hat{C}_T v + \hat{G}_T \qquad (19)$$

where Y is a $4 \times m$ regressor matrix which contains known functions of x, $\dot{x}$, v and a, and $\hat{b}$ is the $m\times1$ vector containing estimates of unknown system parameters. Here it is assumed that the estimates of the forces coming from the patient can be modelled as

$$Y\hat{h} = \hat{F}_p \qquad (20)$$

where Y is the regressor matrix used in Equation 19 and h is the vector of parameters that represent the patient's ability and effort. Furthermore, we define overall system parameters, θ, as $\theta = b - h$ so that

$$Y\hat{\theta} = Y\hat{b} - Y\hat{h} \qquad (21)$$

This relationship represents the difference between forces required to move the patient's limb, and the forces generated by the patient [11], and subsequently a further discussion for both Y and θ will be conducted.

By using Equation 21 and considering that $\ddot{x} = \dot{r} + a$ and $\dot{x} = r + v$, Equation 18 can be written as

$$\begin{aligned} &M_T(x)\dot{r} + C_T(x,\dot{x})r + K_D r = \\ &\tilde{M}_T(x)a + \tilde{C}_T(x,\dot{x})v + \tilde{G}_T(x) - \tilde{F}_p = Y(x,\dot{x},v,a)\tilde{\theta} := \Psi \end{aligned} \qquad (22)$$

where $\tilde{(.)} = \hat{(.)} - (.)$. Next, the adaptation law is defined such that the mapping in Equation 22 from $-r$ to Ψ is passive.

$$\dot{\tilde{\theta}} = -\Gamma^{-1}Y^T r \qquad (23)$$

where $\tilde{\theta}$ is the parameter estimation error and Γ is a symmetric positive definite matrix. Then, by using Equation 22 and 23 the passivity of the mapping from $-r$ to Ψ can be shown as follows:

$$r^T Y\tilde{\theta} = -\dot{\tilde{\theta}}^T\Gamma\tilde{\theta} \qquad (24)$$

hence,

$$\begin{aligned} &-\int_0^t r^T\Psi d\tau = \int_0^t \dot{\tilde{\theta}}^T\Gamma\tilde{\theta}d\tau \\ &= \frac{1}{2}\int_0^t \frac{d}{d\tau}(\tilde{\theta}^T\Gamma\tilde{\theta})d\tau \\ &= \frac{1}{2}\tilde{\theta}^T(t)\Gamma\tilde{\theta}(t) - \frac{1}{2}\tilde{\theta}^T(0)\Gamma\tilde{\theta}(0) \\ &\geq -\frac{1}{2}\tilde{\theta}^T(0)\Gamma\tilde{\theta}(0) \end{aligned} \qquad (25)$$

Please note that the derivative of the parameter estimation error is equal to the derivative of the parameter estimates ($\dot{\tilde{\theta}} = \dot{\hat{\theta}}$), and after defining the adaptation law, the control law can be written in a more compact form as

$$F_r = Y\hat{\theta} - K_D r \qquad (26)$$

The parametrization of both the system dynamics and the forces coming from the patient (Equations 19-21) indicates that the matrix of known functions, Y, consists of both the inertia components, which represent the known functions of the system dynamics, and the components that represent known functions of the patient's ability and effort. The inertia components can be acquired by separating out the linear parameters from the equations of motion. Practically, though, separating these parameters is difficult especially for the systems that include parallel mechanisms in their structure, because of the existence of multiple closed-chains. However, the movements in the rehabilitation of patients with impairments due to neurological lesions are at low speeds and the assumption of being in a quasi-static condition can be made. Consequently, the method proposed in [11] has been adopted and simple models Ia and Iv have been chosen to represent the inertia components of the regressor matrix Y.

Considering that the capability of a patient to apply forces depends on the location of the hand, Gaussian radial basis functions (RBF) are used to model the ability and effort

of the patient. Gaussian RBFs are real-valued functions whose values depend on the distance from the origin [20]. Gaussian RBFs are bounded, strictly positive, and absolutely integrable. Any continuous function, not necessarily infinitely smooth, can be uniformly approximated by linear combinations of Gaussian RBFs [21] which are defined as

$$g_n = \exp(-\|x - \mu_n\|^2/2\sigma^2) \tag{27}$$

where g_n is the n^{th} Gaussian RBF, x is the current location of the RiceWrist's end-effector, μ_n is the location of the n^{th} Gaussian RBF, and σ is a smoothing constant. In total, 80 Gaussian RBFs are assigned to the workspace. We decided the number functions experimentally. Although increasing the number of the functions would enable better approximation, it would also increase the expense of computation. The forces coming from the patient are parameterized using these 80 RBFs. The vector of Gaussian RBFs is defined as

$$g = [g_1 \; g_2 \; ... \; g_{80}]^T \tag{28}$$

Consequently the regressor matrix which represents both the known functions of the system dynamics (simple models Ia and Iv) and known functions of patient's ability and effort (Gaussian radial basis functions) is defined as

$$Y^{4\times 328} = \begin{bmatrix} & & g^T & 0 & 0 & 0 \\ Ia, & Iv, & 0 & g^T & 0 & 0 \\ & & 0 & 0 & g^T & 0 \\ & & 0 & 0 & 0 & g^T \end{bmatrix} \tag{29}$$

The unknown parameter vector θ is a 328×1 vector which is estimated using Equation 23.

III. Results

We present the trajectory tracking performance of the implemented adaptive controller by comparing it with the trajectory tracking performance of a PD controller in simulation, and experimentally using RiceWrist rehabilitation robot. The desired movement, for both simulation and experimental investigation, is chosen as a single axis rotation in the task space to be able to show the performance of different controllers clearly by only altering the controller gains for the given DOF. The movement is a sinusoidal rotation around x_4 (which corresponds to wrist flexion/extension) with a frequency of 0.95 Hz and an amplitude of 0.3 radians (17.2 degrees) and it lasts 9 seconds. The frequency is specified considering the human movement capability. The adaptation gains in Γ are set high in order to achieve a fast adaptation solely for the compactness of the presentation of the results. For rehabilitation applications, lower adaptation gains will be used, in order to grant the patient a proper amount of time required to get acquainted with the modified level of assistance.

A. Simulation

For the simulation, the position and velocity level inverse and forward kinematics, and the forward dynamics equations for the 4-DOF RiceWrist were formulated using Autolev (Online Dynamics), a symbolic manipulator software designed to both derive the equations of motion for multi-body systems by using Kane's method and generate compact C, MATLAB, and Fortran codes for real-time applications [22].

Interaction with subjects was simulated including a, 1 kg virtual load at the end-effector of the mechanism during the formulation of the forward dynamics equations, thus mimicking the situation in which the patient keeps his/her hand relaxed.

We specify 0.6 degrees as the allowable absolute error for the adaptive controller, and the gains (both feedback and adaptation gains) are tuned accordingly. The PD controller used for the comparison uses the same feedback gains. The absolute error values for the both controller, and the corresponding trajectories are given in Fig. 4.

B. Experimentation

In the experimental comparison of the controller performances, the actual RiceWrist prototype is controlled, using a Simulink (The MathWorks, Inc.) software translated into real time code using QuaRC (Quanser Inc.), at a sampling rate of 1 KHz. A healthy subject placed his arm in to the exoskeleton and maintained a relaxed pose throughout the movement. The allowable absolute error is chosen again to be equal to 0.6 degrees, and we applied the same procedure explained in Subsection III-A to tune controller gains. The absolute error values and the corresponding trajectories are given in Fig. 5.

Both the simulation and the experimentation results show that, as desired, the trajectory tracking performance of the adaptive controller is better compared to the performance of a PD controller using the same values of feedback gains. Rather than relying on high feedback gains to drive down error, the adaptive controller learns the model of both the dynamics of the orthosis, and the patient's ability and effort.

IV. Conclusions

We have presented the implementation of a model-based adaptive controller for a serial-in-parallel manipulator, the RiceWrist. The implementation of such a controller requires the development of a dynamical model that can be obtained in a closed analytical form only for a restricted domain of generalized coordinates. Such a domain must be defined in order to prove controller stability. Here, we have applied an existing method to define such domain, and we have verified that the domain of validity of the reduced model is widely within the range of admissible tasks required for the considered application of wrist and forearm rehabilitation. The adaptive controller was implemented in simulation and experimentally on the RiceWrist robot, and trajectory tracking performance was compared to that realized with a proportional-derivative controller. The simulation and the experimental results show that the trajectory tracking performance of the adaptive controller is better compared to the performance of a PD controller using the same values of feedback gains. With the lower gains used in the adaptive controller, good tracking performance is achieved with a

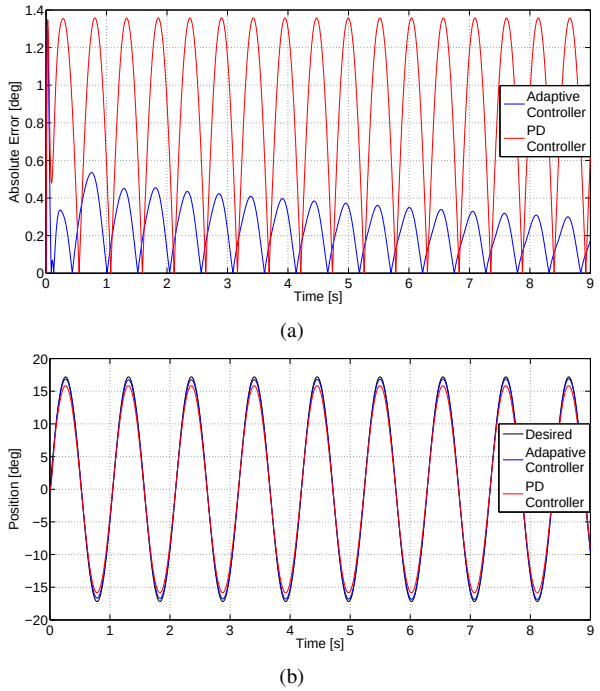

Fig. 4. Absolute error (a) and actual trajectory (b) of both controllers, in simulation, corresponding to the sinusoidal desired rotation around x_4, which corresponds to wrist flexion/extension, with a frequency of 0.95 Hz and an amplitude of 0.3 radians (17.2 degrees).

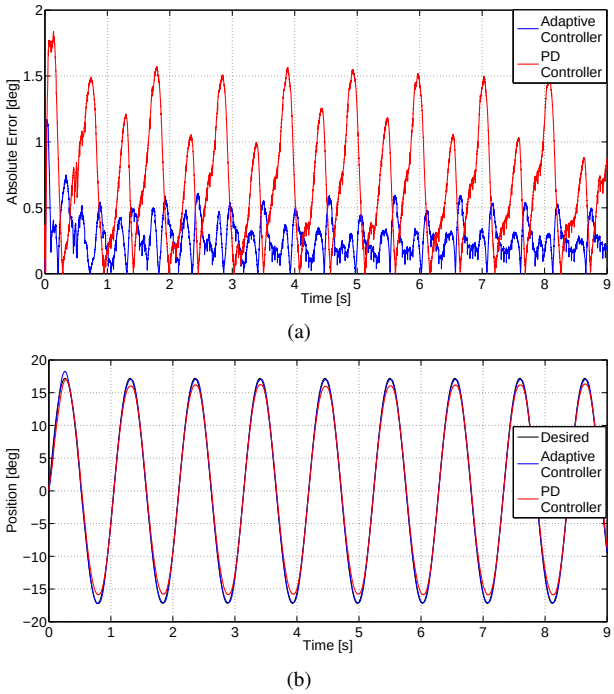

Fig. 5. Absolute error (a) and (b) actual trajectory of both controllers, in experiments, corresponding to the same desired trajectory used in simulation.

more compliant controller that will allow the subject to indicate their ability to independently initiate and maintain movement during a rehabilitation session. We envision to implement a decaying term to bound the assistive forces according to the subject's performance, in a future study.

REFERENCES

[1] R. Riener, T. Nef, and G. Colombo, "Robot-aided neurorehabilitation of the upper extremities," *Medical and Biological Engineering and Computing*, vol. 43, no. 1, pp. 2–10, 2005.

[2] A. Frisoli *et al.*, "Arm rehabilitation with a robotic exoskeleleton in virtual reality," in *Rehabilitation Robotics, 2007. ICORR 2007. IEEE 10th International Conference on*. IEEE, 2007, pp. 631–642.

[3] A. Lo *et al.*, "Robot-assisted therapy for long-term upper-limb impairment after stroke," *New England Journal of Medicine*, vol. 362, no. 19, pp. 1772–1783, 2010.

[4] N. Yozbatiran *et al.*, "Robotic training and clinical assessment of upper extremity movements after spinal cord injury: A single case report," *Journal of Rehabilitation Medicine*, vol. 44, no. 2, pp. 186–188, 2012.

[5] L. Marchal-Crespo and D. Reinkensmeyer, "Review of control strategies for robotic movement training after neurologic injury," *Journal of neuroengineering and rehabilitation*, vol. 6, no. 1, p. 20, 2009.

[6] P. Lum *et al.*, "The MIME robotic system for upper-limb neurorehabilitation: Results from a clinical trial in subacute stroke," in *Rehabilitation Robotics, 2005. ICORR 2005. 9th International Conference on*. IEEE, 2005, pp. 511–514.

[7] D. Feygin, M. Keehner, and R. Tendick, "Haptic guidance: Experimental evaluation of a haptic training method for a perceptual motor skill," in *Haptic Interfaces for Virtual Environment and Teleoperator Systems, 2002. HAPTICS 2002. Proceedings. 10th Symposium on*. IEEE, 2002, pp. 40–47.

[8] N. Hogan *et al.*, "Motions or muscles? Some behavioral factors underlying robotic assistance of motor recovery," *Journal of rehabilitation research and development*, vol. 43, no. 5, p. 605, 2006.

[9] F. Amirabdollahian, W. Harwin, and R. Loureiro, "Analysis of the fugl-meyer outcome measures assessing the effectiveness of robot-mediated stroke therapy," in *Rehabilitation Robotics, 2007. ICORR 2007. IEEE 10th International Conference on*. IEEE, 2007, pp. 729–735.

[10] E. Wolbrecht, "Adaptive, assist-as-needed control of a pneumatic orthosis for optimizing robotic movement therapy following stroke," Ph.D. dissertation, University of California, Irvine, 2007.

[11] E. Wolbrecht *et al.*, "Real-time computer modeling of weakness following stroke optimizes robotic assistance for movement therapy," in *Neural Engineering, 2007. CNE'07. 3rd International IEEE/EMBS Conference on*. IEEE, 2007, pp. 152–158.

[12] R. Sanchez Jr *et al.*, "A pneumatic robot for re-training arm movement after stroke: Rationale and mechanical design," in *Rehabilitation Robotics, 2005. ICORR 2005. 9th International Conference on*. IEEE, 2005, pp. 500–504.

[13] M. OMalley *et al.*, "The ricewrist: A distal upper extremity rehabilitation robot for stroke therapy," in *ASME International Mechanical Engineering Congress and Exposition*, 2006.

[14] L. W. Tsai, "Robot analysis: the mechanics of serial and parallel manipulators," 1999.

[15] F. H. Ghorbel, O. Chételat, R. Gunawardana, and R. Longchamp, "Modeling and set point control of closed-chain mechanisms: theory and experiment," *Control Systems Technology, IEEE Transactions on*, vol. 8, no. 5, pp. 801–815, 2000.

[16] R. Ortega and M. Spong, "Adaptive motion control of rigid robots: A tutorial," *Automatica*, vol. 25, no. 6, pp. 877–888, 1989.

[17] J. Slotine and W. Li, "On the adaptive control of robot manipulators," *The International Journal of Robotics Research*, vol. 6, no. 3, pp. 49–59, 1987.

[18] R. V. Gunawardana, "Control of Serial and Parallel Robots: Analysis and Implementation," *PhD thesis, Rice University*, Aug. 1999.

[19] J. D. Irwin, *The industrial electronics handbook*. CRC, 1997.

[20] M. Buhmann, *Radial basis functions: theory and implementations*. Cambridge Univ Pr, 2003, vol. 12.

[21] F. Girosi and T. Poggio, "Networks and the best approximation property," *Biological Cybernetics*, vol. 63, no. 3, pp. 169–176, 1990.

[22] D. Levinson and T. Kane, "Autolev a new approach to multibody dynamics," *Multibody Systems Handbook. Berlin: Springer: p*, pp. 81–102, 1990.